

See discussions, stats, and author profiles for this publication at: <https://www.researchgate.net/publication/237049544>

Mono-, Di-, and Trinitrenes in the Pyridine Series

ARTICLE *in* JOURNAL OF THE AMERICAN CHEMICAL SOCIETY · MARCH 2000

Impact Factor: 12.11 · DOI: 10.1021/ja9931067

CITATIONS

41

READS

14

4 AUTHORS, INCLUDING:



[Sergei Victorovich Chapyshev](#)

Russian Academy of Sciences

119 PUBLICATIONS **834** CITATIONS

[SEE PROFILE](#)



[Curt Wentrup](#)

University of Queensland

576 PUBLICATIONS **6,470** CITATIONS

[SEE PROFILE](#)

Mono-, Di-, and Trinitrenes in the Pyridine Series

Sergei V. Chapyshev,^{1a} Arvid Kuhn,^{1b} Ming Wah Wong,^{1c} and Curt Wentrup^{*,1b}*Contribution from the Chemistry Department, The University of Queensland, Brisbane, Queensland Qld 4072, Australia**Received August 26, 1999*

Abstract: Tetrafluoro- and tetrachloro-4-pyridylnitrenes are formed on matrix photolysis of the corresponding azides and are found to be highly photostable in low-temperature matrices in contrast to nonhalogenated 4-pyridylnitrene. Matrix photolysis of 3,5-dichloro- or 3-chloro-5-cyano-2,4,6-triazidopyridines leads in rapid succession to mono-, di-, and trinitrenopyridines. The corresponding 3,5-dicyano-2,4,6-triazidopyridine does not produce an identifiable trinitrene. All the above species were identified by evaluation of the temporal evolution of the Ar matrix IR spectra and excellent agreement with DFT-calculated data.

Introduction

While the chemistry of aromatic nitrenes has been investigated in great detail,² that of dinitrenes and trinitrenes is almost unknown. Some meta and para dinitrenes have been observed by ESR spectroscopy,³ but only recently have IR spectra of 4,4'-dinitrenobiphenyl⁴ and *p*-dinitrenobenzene⁵ been reported, and there is only a single previous example of the ESR detection of a trinitrene.⁶ Nitrenes are often generated in quantities sufficient for ESR detection but too small for ready detection by IR spectroscopy⁷ on photolysis of azides. The reason for this is the facile ring expansion of aryl nitrenes to azacyclohepta-1,2,4,6-tetraenes (cyclic ketenimines).^{2,8} This reaction removes the nitrenes and thus make them less useful for photoaffinity labeling purposes.⁹ However, 2,6-difluoro- and pentafluorophenylnitrenes have a higher activation barrier toward ring expansion,¹⁰ and the ring expanded ketenimines have not, in fact, been observed in matrix isolation studies.^{11,12} These fluorinated triplet

nitrenes were stable in Ar matrices, but prolonged irradiation was reported to lead to cyclization to azirines (difluoro- and pentafluoro-7-azabicyclo[4.1.0]hepta-2,4,7-trienes).¹² We have confirmed that these nitrenes are extremely stable toward photolysis in Ar matrices at ca. 10 K, and any secondary reaction was very slow and inefficient under our reaction conditions. For example, in our hands, 2,6-difluorophenylnitrene survives largely unchanged for more than 50 h on photolysis at 444 nm. This property makes the polyfluorinated nitrenes potentially useful for photoaffinity labeling studies. Since highly electrophilic nitrenes react faster in intermolecular reactions, perhalogenated nitrophenylnitrenes or pyridylnitrenes would appear to be particularly desirable for photoaffinity labeling purposes.

In this paper we report the direct matrix-IR spectroscopic observation of nitrenes derived from mono-, di-, and triazides in the perchloro- and perfluoropyridine series.

Results and Discussion

4-Azidotetrafluoropyridine (**1a**) shows major bands at 2136, 1484, and 1218 cm⁻¹ in the IR spectrum in the Ar matrix. UV irradiation (high-pressure Xe/Hg lamp using $\lambda > 290$ nm, or low-pressure Hg lamp without filter (254 nm)) rapidly generates a deep blue matrix containing a new species with major IR absorptions at 1516, 1440, 1417, 1273 (C–N stretch), and 953 cm⁻¹ (Figure 1 and Table 1). Similar irradiation of **1a** in 2-methyltetrahydrofuran glass at 77 K in the cavity of an ESR spectrometer generates a strong nitrene signal at 7029 G ($D = 1.086$; $E \approx 0$ cm⁻¹; microwave frequency 9.2770 GHz). The blue Ar matrix with the IR spectrum as reported above shows a broad absorption band with maxima at $\lambda = 214, 313, 354, 362$, and 371 nm in the UV spectrum and tailing into the visible.

(9) Photoaffinity labeling using aryl nitrenes: Bayley, H.; Knowles, J. R. *Methods Enzymol.* **1977**, *46*, 69. Nielsen, P. E.; Buchardt, O. *Photochem. Photobiol.* **1982**, *35*, 317. Cai, S. X.; Glenn, D. J.; Gee, K. R.; Yan, M.; Cotter, R. E.; Reddy, N. L.; Weber, E.; Keana, J. F. W. *Bioconjugate Chem.* **1993**, *4*, 545. Schnapp, K. A.; Poe, R.; Leyva, E.; Soundararajan, N.; Platz, M. S. *Bioconjugate Chem.*, **1993**, *4*, 172. Tschirret-Guth, R. A.; Ortiz de Montellano, P. R. J. *Org. Chem.* **1998**, *63*, 9711.

(10) Marcinek, A.; Platz, M. S. *J. Phys. Chem.* **1993**, *97*, 12674. Poe, R.; Schnapp, K.; Young, M. J. T.; Grayzer, J.; Platz, M. S. *J. Am. Chem. Soc.* **1992**, *114*, 5054. Karney, W. L.; Borden, W. T. *J. Am. Chem. Soc.* **1997**, *119*, 3347.

(11) Dunkin, I. R.; Thomson, P. C. *J. Chem. Soc., Chem. Commun.* **1982**, 1192.

(12) Morawietz, J.; Sander, W. *J. Org. Chem.* **1996**, *61*, 1, 4351

(1) (a) University of Queensland. Permanent address: Institute of Problems of Chemical Physics, Russian Academy of Sciences, 142432 Chernogolovka, Moscow Region, Russia. (b) University of Queensland. (c) Department of Chemistry, National University of Singapore, Kent Ridge, Singapore 119260.

(2) Scriven, E. F. V., Ed. *Azides and Nitrenes*; Academic Press: New York, NY, 1984. Scriven, E. F. V.; Turnbull, K. *Chem. Rev.* **1988**, *88*, 297. Platz, M. S. *Acc. Chem. Res.* **1995**, *28*, 487. Wentrup, C. *Reactive Molecules*; Wiley: New York, NY, 1984. Wentrup, C. *Adv. Heterocycl. Chem.* **1981**, *28*, 232. Lwowski, W. *Nitrenes*; Wiley: New York, NY, 1970.

(3) (a) Wasserman, E. *Prog. Phys. Org. Chem.* **1971**, *8*, 319. (b) Itoh, K. *Chem. Phys. Lett.* **1967**, *1*, 235. (c) Lahti, P. M.; Minato, M.; Ling, C. *Mol. Cryst. Liq. Cryst. Sci. Technol., Sect. A* **1995**, *271*, 147. Nimura, S.; Yabe, A. Use of Dinitrenes as Models for Intramolecular Exchange. In *Magnetic Properties of Organic Materials*; Lahti, P. M., Ed.; Marcel Dekker: New York, 1999; pp 127–146.

(4) Ohana, T.; Kaise, M.; Yabe, A. *Chem. Lett.* **1992**, 1397.

(5) Nicolaides, A.; Tomioka, H.; Murata, S. *J. Am. Chem. Soc.* **1998**, *120*, 11530. For the corresponding *p*-phenylenebiscarbene, see: Subham, W.; Rempala, P.; Sheridan, S. *J. Am. Chem. Soc.* **1998**, *120*, 11528.

(6) Wasserman, E.; Schueller, K.; Yager, W. A. *Chem. Phys. Lett.* **1968**, *2*, 259.

(7) Examples of matrix IR detection of nitrenes: (a) Phenylnitrene: Hayes, J. C.; Sheridan, S. *J. Am. Chem. Soc.* **1990**, *112*, 5881. (b) 3,5-Bis(trifluoromethyl)-2-pyridylnitrene: Evans, R. A.; Wong, M. W.; Wentrup, C. *J. Am. Chem. Soc.* **1996**, *118*, 4009.

(8) Huisgen, R.; Vossius, D.; Appl, M. *Chem. Ber.* **1958**, *91*, 1. Doering, W. von E.; Odum, R. A. *Tetrahedron* **1966**, *22*, 59. Crow, W. D.; Wentrup, C. *Tetrahedron Lett.* **1968**, 6149. Wentrup, C. *Top. Curr. Chem.* **1976**, *62*, 173. Chapman, O. L.; LeRoux, J.-P. *J. Am. Chem. Soc.* **1978**, *100*, 282. Reisinger, A.; Koch, R.; Wentrup, C. *J. Chem. Soc., Perkin Trans. 1* **1999**, 2247.

Table 1. Calculated and Experimental IR Data for Tetrafluoropyridyl Derivatives **1a**, **3a**, and **2a**

4-azidotetrafluoropyridine ^{a,b} (1a)			4-isocyanatotetrafluoropyridine ^{a,c} (3a)			tetrafluoropyridine-4-nitrene ^{a,b} (2a)		
calcd freq, cm ⁻¹	calcd intens, km/mol	exptl freq, cm ⁻¹	calcd freq, cm ⁻¹	calcd intens, km/mol	exptl freq, cm ⁻¹	calcd freq, cm ⁻¹	calcd intens, km/mol	exptl freq, cm ⁻¹
2270	(734)	2136vs	2361	(1739)	2269vs			
1653	(276)	1641s	1658	(338)	1650 w	1621	(24)	1600w
1628	(15)	1585m	1603	(48)		1536	(265)	1516 + sites m
1516	(242)	1499vs	1496	(667)	1488vs	1439	(602)	1440vs
1493	(655)	1484vvs	1446	(62)	1441s	1421	(68)	1417m
1437	(20)	1429w	1325	(12)				
1354	(50)	1348w				1338	(84)	1328m
1324	(49)	1310w				1290	(44)	1273m ^e
1245	(161)	1218vs	1255	(63)	1249m	1258	(112)	1201m
1012	(156)	1002m	995	(165)	<i>d</i>	1105	(86)	1100m
976	(173)	966m	976	(231)	988	957	(163)	953s
764	(11)	764w				725	(1)	723w
730	(6)	735w				715	(4)	694w
696	(1)	674w				698	(3)	683w
						670	(0)	643/64w
						608	(5)	607w
						595	(3)	582w

^a Unscaled B3LYP/6-311+G* calculations. Most calculated bands with an intensity below 6 km/mol and all bands below 595 cm⁻¹ have been deleted. A full listing as well as scaled and unscaled B3LYP/6-31G* data are given in the Supporting Information. ^b Experimental data in the Ar matrix, ca. 7 K. ^c Experimental data in the Ar/CO matrix, ca. 7 K. ^d Obscured by the azide peak at 1002 cm⁻¹ in the CO matrix. ^e C–N stretching vibration.

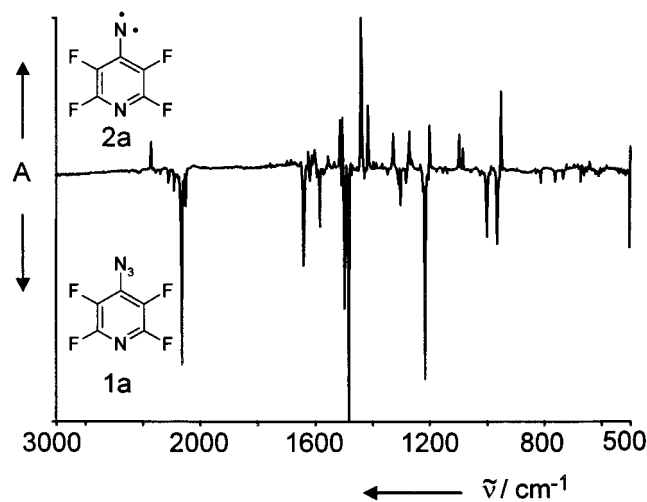
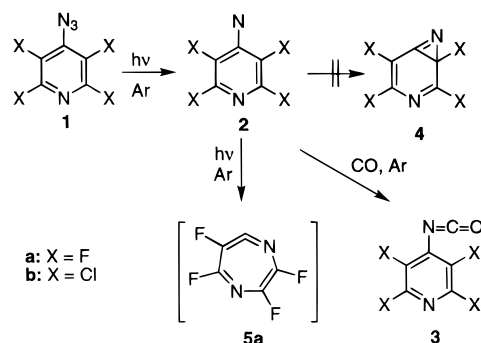


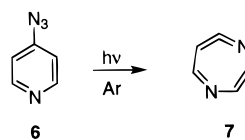
Figure 1. IR difference spectrum showing the photolysis ($\lambda > 290$ nm) of 2,3,5,6-tetrafluoro-4-azidopyridine (**1a**) in argon matrix at 10 K. Bottom: Disappearing bands of **1a**. Top: Appearing bands of nitrene **2a** upon irradiation. The band at 2340 cm⁻¹ is due to CO₂.

The ESR and UV spectra are shown in the Supporting Information. When the photolysis of **1a** was carried out in an Ar matrix containing ca. 10% CO, an isocyanate (**3a**) absorbing strongly at 2269 and 1488 cm⁻¹ was observed (Table 1). This technique has been used successfully to reveal the presence of other nitrenes in matrices.^{4,11,13} All these results make it very reasonable to ascribe the primary photoproduct to tetrafluoropyridylnitrene (**2a**) (Scheme 1). This is further supported by the very good agreement between experimental and calculated IR spectra of both the azide and the nitrene (Table 1). Unscaled DFT-calculated IR spectra at the B3LYP/6-311+G(d) level are in good agreement with experimental data for these and other azides and nitrenes, except that the calculated frequency of the azide stretching vibration at ca. 2100 cm⁻¹ is invariably too high. Very similar values and an even better agreement with experimental data can be obtained using the 6-31G* basis set and different scaling factors for different spectral regions (see

Scheme 1

the section Computational Methods and the Supporting Information). Likewise, for the isocyanate **3a**, there is very good agreement with calculated values, although only the strongest bands were observable experimentally (Table 1).

No cyclization to an azirine **4a** was observed (in contrast to the di- and pentafluorophenylnitrene series¹²). Interestingly, however, a weak absorption at 1869 cm⁻¹ developed during the first 12 min of photolysis and then disappeared. This could possibly be due to ring expansion to the ketenimine **5a**, but this is difficult to prove. The corresponding Ar matrix photolysis of the parent 4-pyridyl azide **6** clearly causes ring expansion to the cyclic ketenimine **7**, absorbing strongly at 1872 cm⁻¹ (eq 1).^{14,15} The calculated wavenumber for ketenimine **7** is 1866



cm⁻¹, and this is the strongest band in the spectrum (B3LYP/6-31G*).¹⁴

(14) Reisinger, A.; Wong, M. W.; Wentrup, C. Unpublished work.

(15) Photolysis of 4-pyridyl azide **6** in Ar matrix gives a nitrene detected by ESR spectroscopy: $D/hc = 1.107$; $E/hc \approx 0$ cm⁻¹. 2-Pyridylnitrene has $D/hc = 1.060$, $E/hc \approx 0$ cm⁻¹; Wentrup, C.; Lüerssen, H.; Kuzaj, M. *Angew. Chem., Int. Ed. Engl.* **1986**, 25, 480. 3-Pyridylnitrene has $D/hc = 1.0048$, $E/hc < 0.003$ cm⁻¹.^{3a}

Table 2. Calculated and Experimental IR Data for Tetrachloropyridyl Derivatives **1b**, **3b**, and **2b**

4-azidotetrachloropyridine ^{a,b} (1b)			4-isocyanatotetrachloropyridine ^{a,c} (3b)			tetrachloropyridine-4-nitrene ^{a,b} (2b)		
calcd freq, cm ⁻¹	calcd intens, km/mol	exptl freq, cm ⁻¹	calcd freq, cm ⁻¹	calcd intens, km/mol	exptl freq, cm ⁻¹	calcd freq, cm ⁻¹	calcd intens, km/mol	exptl freq, cm ⁻¹
2262	(775)	2143/2139/2130m	2363	(1809)	2263vs			
1550	(106)	1528s	1598	(222)	1561m	1487	(11)	1470w
1542	(238)	1513m	1550	(107)		1450	(127)	1421m
1463	(333)	1412s	1536	(77)				
1348	(352)	1332vs	1350	(368)	1338m	1293	(357)	1285vs
1326	(42)		1340	(118)	1321w	1282	(1)	
1270	(13)		1271	(6)		1259	(137)	1247s, 1240m
1210	(60)	1183m	1223	(16)		1207	(174)	1215w
1096	(56)	1100m	1100	(36)		1097	(14)	
903	(62)	905w				971	(90)	974m
879	(16)	888w	890	(109)	920w	884	(5)	892w
740	(2)		750	(1)		723	(1)	721w
738	(123)	750m	708	(144)	718m	681	(111)	691s
635	(26)	648w	622	(3)				
533	(5)	521w	593	(19)				
			582	(20)				

^a Unscaled B3LYP/6-311+G* calculations. Most calculated bands with an intensity below 6 km/mol and all bands below 580 cm⁻¹ have been deleted. A full listing as well as scaled and unscaled B3LYP/6-31G* data are given in the Supporting Information. ^b Experimental data in the Ar matrix, ca. 7 K. ^c Experimental data in the Ar/CO matrix, ca. 7 K.

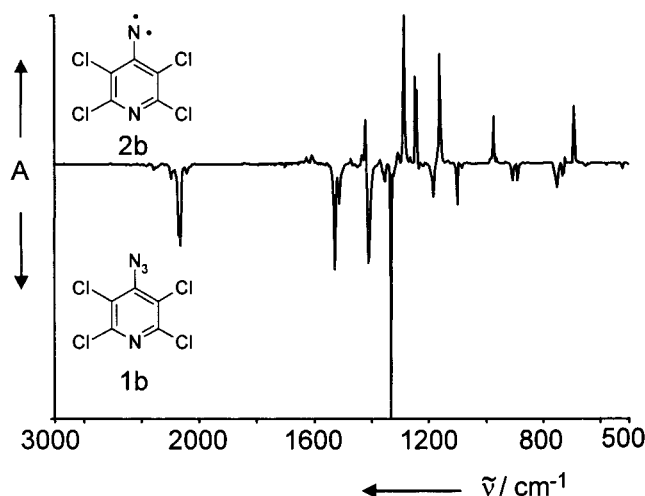


Figure 2. IR difference spectrum showing the photolysis ($\lambda > 290$ nm) of 2,3,5,6-tetrachloro-4-azidopyridine (**1b**) in argon matrix at 10 K. Bottom: Disappearing bands of **1b**. Top: Appearing bands of nitrene **2b** upon irradiation.

Tetrachloro-4-pyridylnitrene (**2b**) was generated by analogous photolysis of azide **1b** (Scheme 1, Figure 2). The azide has strong IR absorptions at 2143, 1412, and 1332 cm⁻¹, and nitrene **2b** at 1421, 1285, 1247, and 691 cm⁻¹ (Table 2). This deep blue nitrene is again trappable with CO to give an isocyanate (**3b**) (Table 2). The ESR spectrum of the nitrene was obtained in 2-methyltetrahydrofuran glass at 77 K and shows $D = 1.040$ and $E \approx 0$ cm⁻¹. The UV spectrum of the Ar matrix is shown in the Supporting Information. There was no evidence for the formation of an azirine **4b** or ketenimine **5b** in the Ar matrix; no new species was formed on extensive photolysis, but the starting azide **1b** was slowly regenerated in the course of photolysis at 444 nm for 12 h. This can be explained by trapping of the nitrene by molecular nitrogen. This phenomenon has also been observed in the case of phenyl nitrene.^{7a} Again, there is good agreement between experimental and calculated IR spectra of **1b**, **2b**, and **3b** (Table 2).

Photolysis of Matrix Isolated Diazides 8a,b. As a prelude to the photolysis of triazidopyridines to produce mono-, di-, and trinitrenes, we examined the photolysis of the 2,6-diazides **8a,b**, which can only give rise to mono- and dinitrenes. In fact,

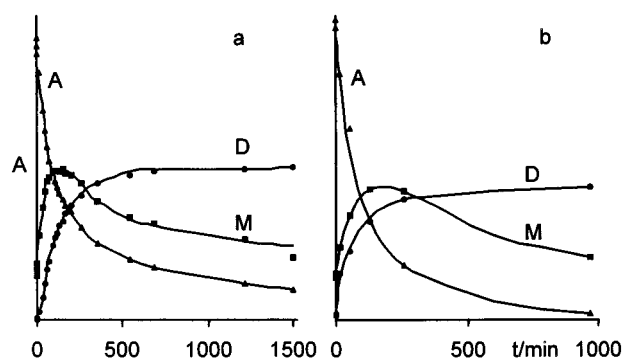
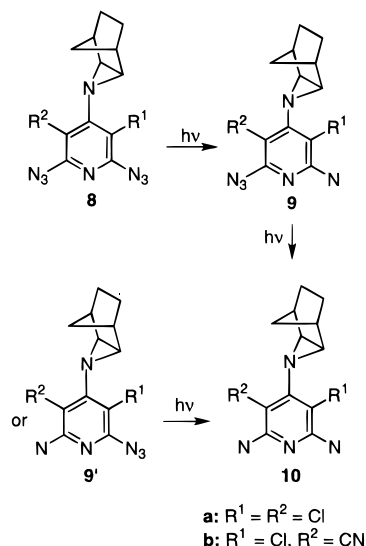


Figure 3. Course of the photolyses of matrix-isolated (argon, 7 K) diazidopyridines **8a** (a) and **8b** (b) with light of wavelength $\lambda > 350$ nm as derived from the integration of representative IR bands which are assigned to the corresponding azides A, mononitrenes M, and dinitrenes D. The bands used for integration in the figure are 1194 (azide), 1474 (mononitrene), and 1315 (dinitrene) cm⁻¹ for **8a** and 1193 (azide), 1475 (mononitrene), and 1152 (dinitrene) cm⁻¹ for **8b**. The ordinates for the plot of the dinitrenes D are expanded by a factors of 10 (a) and 4 (b), respectively.

long-wavelength photolysis (>350 nm) caused a steady decrease in the absorptions of the matrix-isolated diazides, which were almost completely converted to new products in the course of ca. 24 h. Purple matrices formed, with sets of new bands increasing in intensity to reach a maximum after ca. 2 h of photolysis, whereupon they decreased and finally disappeared. The full data are reported in the Supporting Information, and illustrated in Figure 3. Since the final product does not contain azido groups, we assume that the intermediate product is due to the mononitrenes in the 2- and/or 6-position (**9**, **9'**), and the final product is the 2,6-dinitrene (**10**). In agreement with this view, the formation of ESR signals due to mono- and dinitrenes was observed under similar irradiation conditions in 2-methyltetrahydrofuran glasses at 77 K.¹⁶

Photolysis of Triazide 11a (Cl/Cl-Substituted). The IR spectrum of triazide **11a** in the Ar matrix is depicted in Figure 4 and in the Supporting Information. The strongest absorptions are at 2150vs, 2131m, and 1387vs cm⁻¹ (Table 3). The IR spectrum of this triazide was calculated at the B3LYP/6-31G* level (scaled), whereas the nitrenes were calculated at the

Scheme 2



6-311G* level (unscaled values in Table 3). It is seen in Table 3 that there are, in some instances, two or three experimental bands for each calculated frequency. This is readily explained in terms of multiple sites and/or the existence of more than one conformer of the triazide in the matrix. Only the calculated IR spectrum of the lowest energy conformer is given. This is planar and has the 2- and 6-azido groups “down”, parallel to the nitrogen lone pair (Z,Z; the calculated structures are given in Figure S6 in the Supporting Information). The corresponding conformer with the 2-azido group “up” (E,Z) has only slightly higher energy, and the calculated IR spectrum does not differ much from the one listed. Likewise, mono- and dinitrenes can have the 2,6-azido groups “down” (Z) (data given in Table 3) or “up” (E). The IR spectra of the conformers with a 2- or 6-azido group “up” (E) were calculated, but as they do not differ a great deal from the ones tabulated, they are not listed in Table 3.

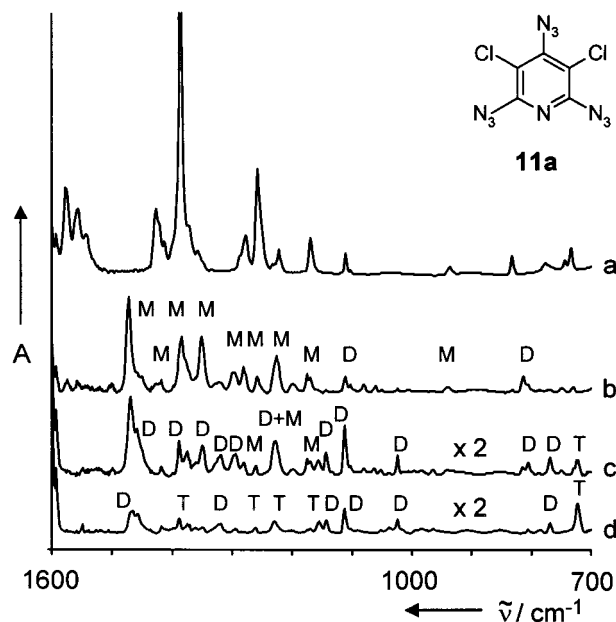
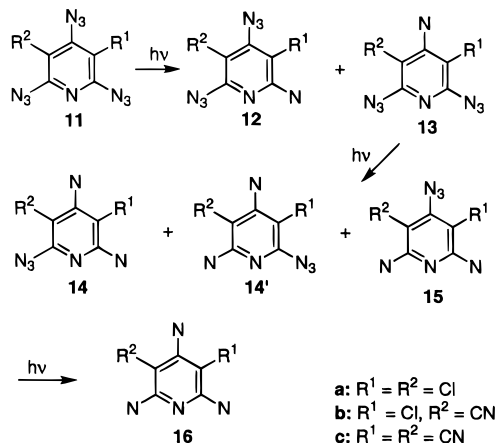


Figure 4. IR spectra of the photolysis of matrix-isolated triazidopyridine **11a** with $\lambda = 334$ nm: (a) starting material **11a**; (b) after 150 min irradiation, mainly mononitrenes **12/13a**; (c) after 15 h, mainly dinitrenes **14a/15a**; and (d) after 26 h, trinitrene **16a**. Letters denote bands assigned to M mononitrenes, D dinitrenes, and T trinitrene. The ordinates in parts c and d are expanded by a factor of 2.

Scheme 3



The matrix photolysis of **11a** was carried out under a variety of conditions: (i) broad-band irradiation with the Xe/Hg high pressure lamp; (ii) monochromatically at 313 nm; (iii) $\lambda > 320$ nm; and (iv) monochromatically at 335 nm.

Photolysis of **11a** for 1 min at 335 nm gave rise to a series of new peaks, including signals in the 2100 cm^{-1} region, thus indicating that the new product still contains azido groups. The values are compared with calculated values for the two possible mononitrenes, **12a** and **13a**, in Table 3. The calculated spectra of the two mononitrenes do not differ a great deal, and it would be impossible to make a choice between them on this basis alone. However, the ESR spectrum obtained under the same irradiation conditions in 2-methyltetrahydrofuran glass at 77 K clearly indicates that two mononitrenes are formed within 1 min and absorbing at 6694 and 7036 G.¹⁷ The dominant lower field signal is ascribed to the 2-nitrene, and the weaker higher field signal to the 4-nitrene.^{15–17} With this knowledge, it is seen that the IR spectrum agrees well with a mixture of the two mononitrenes (Table 3). Continued photolysis for 2–7 min at 335 nm, for 80 s at >320 nm, or for 20 s with broad band irradiation caused an increased formation of the nitrene, but no new species according to IR spectroscopy. However, irradiation at 313 nm was less selective: after 90 s, there was absorption of the two nitrenes **12a** and **13a** as above, together with new signals ascribed to a mixture of dinitrenes **14a** and **15a**. Comparison of the new peaks with calculated values for the two dinitrenes in fact indicates that both are present (Table 3).

The spectrum of the dinitrenes was extracted by subtraction of the IR spectra of the products of two different photolyses, (i) one containing mainly mononitrenes **12a/13a**, obtained after broad band irradiation of the azide for 1.5 min, and (ii) one containing mainly **14a/15a**, obtained after 6 min of broad band irradiation. This spectrum is also obtained on irradiation of the triazide at 335 nm for 70 min and subtracting the spectrum resulting after 1 min (the mononitrenes).

It is known from ESR spectroscopy that a septet trinitrene forms after 4 min of irradiation of **11a** (77 K, MTHF, $\lambda > 290$ nm).¹⁶ Therefore, we may expect the IR signals of **16a** in admixture with those of **12a** and **13a** after 10–30 min of irradiation of **11a**. From an analysis of the spectra obtained between 7 and 70 min at 335 nm, new bands that can be assigned to **16a** are given in Table 3, where they are compared with the calculated values for this species.

The evolution of the azide and mono-, di-, and trinitrenes is illustrated in Figures 4 and 5. By careful monitoring of the full

(17) For the ESR investigation of the triazides described in this paper, see: Chapyshev, S. V.; Walton, R.; Sanborn, J. A.; Lahti, P. M. *J. Am. Chem. Soc.* **2000**, *122*, 1580–1588.

Table 3. Calculated and Experimental IR Data for 3,5-Dichlorotriazidopyridine (**11a**)

triazide 11a		2-nitrene 12a		4-nitrene 13a	2,4-dinitrene 14a		2,6-dinitrene 15a	2,4,6-trinitrene 16a	
calc ^{a,b} ν (int)	exptl ν	calc ^{c,d} ν (int)	exptl ν	calc ^{c,d} ν (int)	calc ^{c,d} ν (int)	exptl ν	calc ^{c,e} ν (int)	calc ^{c,e} ν (int)	exptl ν
	2237m, 2216w, 2201vw	2280 (604)	2158 s	2280 (1284)	2280 (677)	2199, 2134	2266 (677)		
2163 (896)	2186m	2262 (914)	2131s, 2118s	2264 (175)					
2149 (160)	2150vs								
2144 (1102)	2131m, 2099m								
1535 (70)	1577m, 1559m, 1555m, 1544m	1524 (119)	1501w	1539 (214)	1469 (278)	1471s, 1460m	1481 (382)		
1456 (164)	1427m, 1421w	1496 (402)	1473vs	1476 (239)	1394 (222)	1389s	1403 (87)	1371 (23)	1390m
1403 (530)	1414w	1434 (233)	1451w, 1419w	1406 (456)	1349 (260)	1376m, 1360w, 1350m	1384 (9)	1333 (15)	
1400 (564)	1387vs	1373 (530)	1385s	1362 (381)	1316 (45)	1320ms	1319 (12)	1304 (15)	1263w
1320 (65)	1374w	1344 (85)	1352s	1293 (34)	1304 (4)	1295m	1302 (30)	1276 (10)	1230w
1295 (57)	1358vw	1281 (7)	1298m, 1281w	1276 (93)	1270 (3)	1261w	1261 (50)	1188 (27)	
1279 (36)	1289w, 1278m	1262 (32)	1260m, 1227s	1267 (2)	1239 (42)	1229s	1203 (9)	1124 (78)	1156w
1204 (24)	1258m, 1233w, 1223w, 1169m	1241 (12)	1200w, 1176m, 1170w	1223 (582)	1144 (50)	1145m, 1113vs	1122 (93)	1030 (47)	1038vw
1090 (33)	1111w, 1103vw	1087 (26)	1080w	1109 (54)	1064 (34)	1064w, 1053w	1064 (10)	761 (67)	723s
956 (30)	937w	1076 (20)	1061w	1031 (31)	1017 (42)	1025m, 1005w	980 (33)	708 (8)	
829 (37)	833m	949 (41)	940w		805 (61)	805m	792 (65)		
775 (39)	778w	803 (78)	814m	830 (32)	733 (37)	770m	725 (12)		
752 (16)	745w	787 (23)	749w, 730w	754 (22)	716 (9)	707vw, 692vw	692 (2)		
741 (46)	734m	729 (10)	694w	699 (41)	620 (5)		627 (4)		
583 (5)	585vw	636 (17)			575 (9)		585 (4)		
551 (18)	545vw	567 (12)	547 w	550 (14)	565 (7)		523 (7)		
528 (8)	527vw	525 (4)			539 (5)		500 (5)	401 (11)	
		376 (8)		366 (5)	392 (6)		403 (6)	387 (8)	
					377 (5)		374 (8)	311 (4)	
					315 (5)		314 (3)	252 (3)	
					198 (4)		192 (5)	187 (8)	

^a B3LYP/6-31G* calculated frequencies scaled by 0.94 ($>2000\text{ cm}^{-1}$), 0.98 ($2000\text{--}1000\text{ cm}^{-1}$), and 1.00 ($<1000\text{ cm}^{-1}$) (intensities in km/mol).

^b Bands with calculated intensities $<5\text{ km/mol}$ have been deleted. ^c B3LYP/6-311+G* calculations, unscaled. ^d Bands $<4\text{ km/mol}$ deleted. ^e Bands $<2\text{ km/mol}$ deleted.

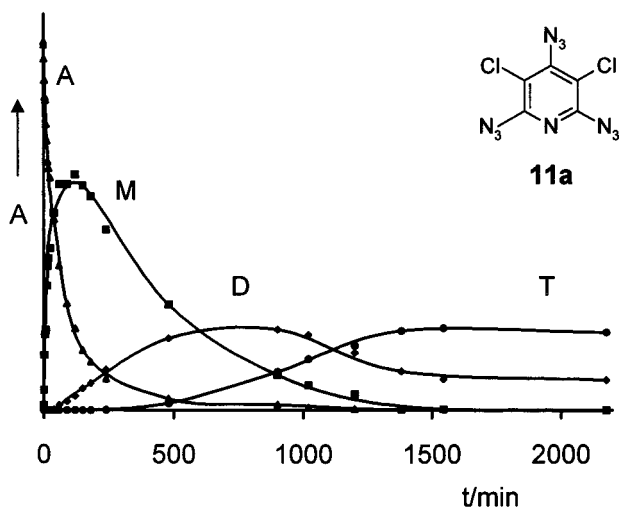


Figure 5. Course of the photolysis of matrix-isolated (argon, 7 K) triazidopyridine **11a** with light of wavelength $\lambda = 334\text{ nm}$ as derived from the integration of representative IR bands which are assigned to A azide **11a**, M mononitrenes **12/13a**, D dinitrenes **14a/15a**, and T trinitrene **16a**. The bands used for integration in the figure are 833 (azide), 814 (mononitrenes), 805 (dinitrenes) and 723 (trinitrene) cm^{-1} . The ordinate for the plot of the trinitrene T is compressed by a factor of 4.

spectra during 2 days of photolysis at 335 nm, it was possible to plot the temporal development of all the species. Strong, characteristic peaks for each species were selected for the construction of Figure 5, but analogous evolution is observed for several other peaks ascribed to each species. This is illustrated further in the Supporting Information. Since peak heights are used without a knowledge of extinction coefficients,

the ordinates in Figure 5 are on arbitrary and variable scales. The abscissa time scale is longer here than in the text because a weaker lamp and a longer water filter were used, causing slower photolysis.

Septet **16a** is formed in a low concentration only, and it is photochemically unstable, disappearing after 13 min of broad band irradiation. The photochemical destruction of all azides and nitrenes in the matrix by using broad band photolysis from the beginning gave rise to new bands at 2300, 2255, 2050, 1960, and 1802 cm^{-1} (possibly nitriles, ring expanded carbodiimide, and ketenimines), all appearing in the course of 30 min.

Photolysis of Matrix-Isolated Triazide 11b (Cl/CN-Substituted). Azide **11b** was photolyzed in Ar matrix using the same conditions as for **11a**. In all cases, even very brief photolysis caused formation of new products and a deep blue matrix (e.g. in 20 s with broad band, or 5 min with 335 nm irradiation). Observed and calculated bands of two conformers of the azide and the two possible mononitrenes (**12b** and **13b**) and dinitrenes (**14b** and **15b**) are given in Table 5. The spectra of the mononitrenes and the dinitrenes were extracted by difference spectroscopy, e.g. by subtraction of the spectrum resulting after 20 min of irradiation at 335 nm (mainly mononitrene mixture) from that after 40 min (mainly dinitrene mixture). The good agreement with calculated values supports the assignment of these mono- and dinitrenes. This is also in accord with the ESR spectra.¹⁶

By IR spectroscopy, the dinitrene mixture persists after 13 h at 335 nm, but the difference spectra obtained after this time indicated that a major new species, assigned as the septet trinitrene **16b**, had formed. Again, the good agreement between experimental and calculated spectra of all the species supports the assignments (Table 4).

Table 4. Calculated and Experimental IR Data for 3-Chloro-5-cyanotriazidopyridine (**11b**)

triazide 11b			2-nitrene 12b		4-nitrene 13b	6-nitrene 13'b	2,4-dinitrene 14b		4,6-dinitrene 14'b	2,6-dinitrene 15b	2,4,6-trinitrene 16b	
calc ^{a,c} ν (int)	calc ^{a,c,d} ν (int)	exptl ν	calc ^{a,c} ν (int)	exptl ν	calc ^{a,c} ν (int)	calc ^{a,e} ν (int)	calc ^{a,c} ν (int)	exptl ν	calc ^{a,c} (int)	calc ^{a,e} ν (int)	calc ^{a,c} ν (int)	exptl ν
2201 (36)	2208 (14)	2253w, 2235w 2000w	2184 (1)	2230w, 2224w	2196 (1)	2189 (1)	2165 (585)	2136vs	2166 (172)	2173 (1)	2150 (11)	
2165 (1036)	2166 (906)	2153vs, 2143s	2165 (466)	2162s	2166 (1148)	2166 (576)	2156 (34)		2165 (458)	2149 (619)		
2152 (176)	2153 (165)	2131s	2148 (899)	2122s	2153 (185)	2147 (771)						
2145 (817)	2146 (1047)	2114w, 2083w	1516 (23)	1505s, 1512s, 1521s, 1545s	1515 (304)	1504 (338)	1455 (302)	1452vs, 1415vs	1454 (365)	1468 (425)		
1564 (599)	1561 (483)	1584m, 1576m, 1561s	1472 (799)	1466vs	1460 (264)	1470 (269)	1381 (178)	1353s	1388 (132)	1400 (41)	1372 (4)	1328s, 1340w
1530 (293)	1538 (316)	1545s, 1529w, 1522w, 1513w, 1505w	1423 (34)	1408s, 1416s	1410 (445)	1417 (310)	1333 (132)	1345m	1358 (271)	1365 (8)	1329 (8)	1320w
1448 (99)	1453 (244)	1427 s	1375 (437)	1364s, 1353s, 1347s, 1340m	1363 (389)	1392 (235)	1318 (113)	1292m	1303 (95)	1299 (34)	1312 (8)	1292w
							1284 (17)		1284 (18)	1252 (48)	1299 (26)	1258vs
1417 (567)	1416 (590)	1416 m	1309 (60)	1307w	1282 (27)	1332 (268)	1262 (11)				1269 (18)	1252m
1402 (541)	1405 (466)	1401s, 1395vs, 1382s, 1366w, 1375w, 1354w	1305 (61)	1304 w	1256 (137)	1279 (25)	1230 (51)	1205m		1202 (8)	1190 (10)	
							1184 (18)	1194w, 1153w, 1144s	1140 (69)	1160 (17)	1178 (20)	1174m
1326 (70)	1322 (175)	1347w, 1340w	1253 (36)	1222 s	1238 (205)	1254 (5)	1061 (43)	1041w, 1058w	1112 (12)	1077 (45)	1116 (34)	1131m
1298 (233)	1298 (13)	1301w, 1283w	1215 (35)	1219 s		1213 (7)	1027 (12)		1007 (37)	989 (21)	1040 (40)	986m
1288 (24)	1289 (48)	1253s, 1230w	1138 (25)	1130 w	1148 (118)	1149 (26)	846 (32)		846 (59)	858 (31)	821 (37)	810w
1203 (48)	1203 (20)	1196w, 1183w, 1174w	1067 (9)	1060 w		1064 (21)	758 (19)	730w, 721w	721 (11)	737 (11)	719 (10)	725m
1165 (20)	1162 (28)	1145w	973 (19)	1013 w	1017 (15)	962 (38)	727 (9)					
969 (35)	962 (20)	948w, 943w, 936w	861 (38)		874 (23)	868 (57)						
877 (26)	880 (38)	907w, 901w, 871w, 843w	780 (35)	772 w								
797 (32)	804 (28)	793w, 781w	750 (11)	728 w	755 (15)	743 (13)	654 (9)					
762 (16)	766 (15)	769w, 760w			750 (13)		587 (10)			525 (7)		
750 (19)	751 (25)	745w		715 w	742 (27)		555 (9)		556 (9)	514 (7)		
552 (14)	553 (14)	545w	636 (7)	636 w		639 (12)	237 (10)		319 (14)		396 (12)	
540 (11)	532 (9)	525w	562 (12)		550 (13)	558 (10)			197 (11)	191 (10)	187 (13)	

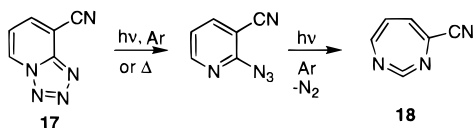
^a B3LYP/6-31G* calculated frequencies scaled by 0.94 ($>2000\text{ cm}^{-1}$), 0.98 ($2000\text{--}1000\text{ cm}^{-1}$), and 1.00 ($<1000\text{ cm}^{-1}$) (intensities in km/mol). ^b Lowest energy conformer: 2-azide down, 4-azide left, 6-azide down (see Figure S6). ^c Bands with calculated intensities $\leq 8\text{ km/mol}$ have been deleted. ^d Second-lowest energy conformer: 2-azide down, 4-azide right, 6-azide right (see Figure S6). ^e Bands $\leq 6\text{ km/mol}$ deleted.

Table 5. Calculated and Experimental IR Data for Dicyanotriazidopyridine **11c**

triazide 11c		2-nitrene 12c		4-nitrene 13c	2,4-dinitrene 14c		2,6-dinitrene 15c
calc ^{a,b} ν (int)	exptl ν	calc ^{a,b} ν (int)	exptl ν	calc ^{a,c} ν (int)	calc ^{a,d} ν (int)	exptl ν	calc ^{a,e} ν (int)
2211 (9)	2285w, 2273w	2190 (0)	2190w	2195 (0)			2175 (7)
2203 (34)	2236w	2185 (8)	2151w	2194 (0)			2172 (9)
2167 (1005)	2161vs, 2179m	2167 (588)	2120m	2168 (1116)	2168 (591)	2138m	2149 (502)
2155 (171)	2156vs	2148 (615)		2156 (193)	2165 (2)		
2147 (779)	2145s, 2141s, 2134s, 2129s				2155 (31)		
1561 (345)	1584m, 1577m, 1565s		1506m	1509 (355)			
1545 (716)	1554vs	1519 (185)	1520m				
1447 (131)	1431vs	1471 (458)	1486vs	1462 (288)	1456 (343)	1423w, 1455m, 1472w	1459 (412)
1428 (708)	1412m	1407 (410)	1457s	1420 (518)	1390 (176)	1386w	1411 (70)
1408 (457)	1407m	1396 (208)	1387s, 1373s	1380 (351)	1357 (167)	1354w	1356 (6)
1328 (165)	1398vs	1332 (202)	1363w		1316 (119)		1348 (6)
1303 (161)	1299m	1307 (35)		1283 (9)	1281 (13)	1301w	1306 (34)
1291 (25)	1271m	1261 (31)	1218m	1272 (64)	1270 (26)	1266w	
1225 (26)	1249, 1226m, 1220m	1204 (6)		1240 (324)	1248 (12)	1225w	1255 (49)
1183 (10)	1206s, 1144m	1177 (54)	1200w	1188 (11)	1192 (37)	1199w	1204 (7)
1063 (7)				1056 (14)		1159w	1164 (10)
976 (20)	950w	974 (45)			1115 (15)	1148w	1148 (23)
930 (12)					1034 (23)	1058w, 1035w	980 (19)
823 (24)	811w			773 (18)	893 (15)		915 (9)
777 (15)	773m	756 (11)	759w	761 (12)	776 (9)		
755 (14)				757 (12)	737 (8)		
635 (13)	629w	661 (14)	658w		660 (7)	740w	747 (10)
553 (15)	547w, 552w	559 (7)	539w	550 (17)			
532 (10)		537 (7)			556 (9)		
				212 (10)	231 (11)		191 (11)
					197 (11)		

^a B3LYP/6-31G* calculated frequencies scaled by 0.94 ($>2000\text{ cm}^{-1}$), 0.98 ($2000\text{--}1000\text{ cm}^{-1}$), and 1.00 ($<1000\text{ cm}^{-1}$). Calculated intensities in parentheses (km/mol). ^b Calculated bands with intensities $<7\text{ km/mol}$ deleted. ^c Bands $<10\text{ km/mol}$ deleted. ^d Bands $<7\text{ km/mol}$ deleted. ^e Bands $<6\text{ km/mol}$ deleted.

Photolysis of Matrix-Isolated Triazide **11c (CN/CN-Substituted).** Irradiation of matrix-isolated azide **11c** for 12 min at 313 nm or for 2 min at 313 nm gave rise to new bands, inter alia 2190w, 2151w, 2120m, 2002w, 1521m, 1506m, 1468vs, 1457s, 1387s, 1373s, 1363w, 1218m, 1200w, 759w, 658w, and 539w. Comparison with the calculated values suggests that again we have a mixture of mononitrenes **12c** and **13c** (Table 5), except that the weak band at 2002 does not fit the calculations and suggests that some ring expansion to a seven-membered ring carbodiimide takes place in the beginning of the photolysis, similar to the case of **1a** described above. This band disappeared on further photolysis at 313 nm for 1 h, or with $\lambda > 290\text{ nm}$ for 15 min. Ar matrix photolysis of 3-cyano-2-azidopyridine (8-cyanotetrazolo[1,5-*a*]pyridine, **17**) readily gives rise to the ring-expanded carbodiimide **18** (eq 2).¹⁸



Further changes taking place on irradiation at 313 nm allow the assignment of signals to the two mononitrenes (**14c** and **15c**) (Table 5). After 50 min, the mononitrenes and the dinitrenes have roughly equal intensities. After 75 min the dinitrene mixture dominated. It should be noted that all these new peaks (mono- and dinitrenes) account for only ca. 1% of the intensity of the starting azide **11c**. However, two additional new band at 2180vs and 2090vs cm^{-1} after the 75 min irradiation show more than 100% of the intensity of the starting azide, thus indicating that the main photoproduct in this case is not the trinitrene but a ring-expanded carbodiimide-type compound. A number of plausible structures can be written, including didehydrotriazolo-

cines with an azide substituent or an annelated azirine ring and containing both ketenimine and carbodiimide functionalities, or even a tridehydrotetraazone and compounds derived from such structures. This photoproduct was stable to further irradiation $>290\text{ nm}$. A further photounstable product absorbing at 2152 cm^{-1} was also obtained in the 75 min photolysis. These unknown compounds possess weak CN group absorptions in the $2244\text{--}2255\text{ cm}^{-1}$ region. Thus, triazide **11c** behaves differently from the other two. The formation of ring-expansion products of unknown structure explains why no septet trinitrene was observed by ESR in this case.¹⁶

Conclusion

Halogenated pyridyl nitrenes are relatively long-lived under matrix conditions. Mono-, di-, and trinitrenes in this series are clearly identifiable by IR spectroscopy. Such identification is aided very strongly by the mostly excellent agreement between experimental and DFT-calculated IR spectra. It is worth noting that the spectral assignments were mostly made before the computational data were available for comparison and verification. The interpretations based on IR spectroscopy are also strongly supported by the corresponding ESR observations reported from Lahti's laboratory.¹⁷

Computational Method

Density functional theory calculations were performed using the Gaussian 94 or Gaussian 98 suites of programs.¹⁹ B3LYP (UB3LYP for nitrenes)/6311+G* calculations of IR spectra are used without scaling factors and give good agreement with experiment $<2000\text{ cm}^{-1}$. The 6-31G* basis set gave frequency values almost identical with those of the larger basis set, provided scaling factors were used; excellent agreement with experiment was achieved throughout the spectral range by using the following scaling factors: 0.94 ($>2000\text{ cm}^{-1}$), 0.98 ($2000\text{--}1000\text{ cm}^{-1}$), and 1.00 ($<1000\text{ cm}^{-1}$). Some data obtained with the

(18) Addicott, C.; Wentrup, C. Unpublished results.

unscaled 6-311+G* basis and the scaled and unscaled 6-31G* basis sets are presented in the Supporting Information for illustration. Since the calculation of all the species described in this paper using the larger basis set was prohibitive, some spectra were only calculated at the 6-31G* level, using the scaling factors mentioned. Only triplet, quintet, and septet nitrenes were considered due to the ESR spectroscopic findings. Only the IR spectra of the lowest energy conformers of azide-containing species were calculated; the energy ordering was based on fully optimized geometries.

Experimental Section

Materials. Monoazides **1a**²⁰ and **1b**,²¹ diazides **8**,^{22,23} and triazides,^{23,24,25} **11a–c** were prepared according to literature procedures.

Ar matrices were prepared by vacuum deposition of samples with Ar at ca. 20 K using APD Cryogenics liquid He cryostats DE202 and CSW-204SL-6.5K. Ar/CO matrices contained ca. 10% CO. IR and UV spectra were recorded at ca. 7 K using Perkin-Elmer 2000 and Varian Cary 1 spectrometers, respectively. ESR spectra were recorded on a Bruker ER2000 spectrometer at ca. 15 K in Ar matrices or at 77 K in

(19) Gaussian 98, Revision A.6; Frisch, M. J., Trucks, G. W., Schlegel, H. B., Scuseria, G. E., Robb, M. A., Cheeseman, J. R., Zakrzewski, V. G., Montgomery, J. A., Jr., Stratmann, R. E., Burant, J. C., Dapprich, S., Millam, J. M., Daniels, A. D., Kudin, K. N., Strain, M. C., Farkas, O., Tomasi, J., Barone, V., Cossi, M., Cammi, R., Mennucci, B., Pomelli, C., Adamo, C., Clifford, S., Ochterski, J., Petersson, G. A., Ayala, P. Y., Cui, Q., Morokuma, K., Malick, D. K., Rabuck, A. D., Raghavachari, K., Foresman, J. B., Cioslowski, J., Ortiz, J. V., Stefanov, B. B., Liu, G., Liashenko, A., Piskorz, P., Komaromi, I., Gomperts, R., Martin, R. L., Fox, D. J., Keith, T., Al-Laham, M. A., Peng, C. Y., Nanayakkara, A., Gonzalez, C., Challacombe, M., Gill, P. M. W., Johnson, B., Chen, W., Wong, M. W., Andres, J. L., Gonzalez, C., Head-Gordon, M., Replogle, E. S., and Pople, J. A.; Gaussian, Inc.: Pittsburgh, PA, 1998.

(20) Banks, R. E. *J. Chem. Soc., Perkin Trans. 1* **1972**, 2964.

(21) Bernard, I. R. A.; Chivers, G. E.; Cremllyn, R. J. W.; Mootoosamy, K. G. *Aust. J. Chem.* **1974**, 27, 171.

(22) Chapyshev, S. V.; Ibata T. *Heterocycles* **1993**, 36, 2185.

(23) Chapyshev, S. V. *Mendeleev Commun.* **1999**, 164.

(24) Chapyshev, S. V. *Khim. Geterotsikl. Soedin.* **1993**, 1650. Chapyshev, S. V. *Chem. Heterocycl. Compd.* **1993**, 29, 1426.

2-methyltetrahydrofuran glasses in suprasil tubes as specified in the text. Photolyses were carried out using a 1000 W Hanovia Xe/Hg lamp and a monochromator for specific wavelengths or cutoff filters for wavelength ranges ($\lambda > x$ nm). General procedures for matrix isolation and photolysis experiments have been published previously.^{7b,26}

Acknowledgment. This work was supported by the Australian Research Council (all experimental and some computational work) and the National University of Singapore (computational facilities). We are further indebted to Dr Hiroyuki Niino, National Institute of Materials and Chemical Research, Tsukuba, Japan, for helping to perform many of the large-scale computations. We thank Professor Paul Lahti, University of Massachusetts, Amherst, for sharing with us the results of the ESR investigations in his laboratory prior to publication.

Supporting Information Available: UV spectra of **2a** and **2b**, ESR spectrum of **2a**, IR data for **8–10a,b**, and temporal evolution of the spectra; calculated structures of the lowest energy conformers of **11–15a** (B3LYP/6-31G*); difference spectrum showing azide **11a** and mononitrenes **12/13a**, and temporal evolution of peaks due to azide and mono-, di-, and trinitrenes (**11a–16a**); B3LYP/6-31G* and 6-311+G* calculations of IR spectra for **1a,b**, **2a,b**, and **16b**; B3LYP/6-31G* calculations for **16c**; and calculated total energies and S^2 values for **11–16a–c** (B3LYP/6-31G*) (PDF). This material is available free of charge via the Internet at <http://pubs.acs.org>.

JA9931067

(25) Chapyshev, S. V.; Bergstrasser, U.; Regitz, M. *Khim. Geterotsikl. Soedin.* **1996**, 67. Chapyshev, S. V.; Bergstrasser, U.; Regitz, M. *Chem. Heterocycl. Compd.* **1996**, 32, 59.

(26) Qiao, G. G.; Andraos, J.; Wentrup, C. *J. Am. Chem. Soc.* **1996**, 118, 5634 and references therein.